

This is an Open Access document downloaded from ORCA, Cardiff University's institutional repository: <https://orca.cardiff.ac.uk/id/eprint/95486/>

This is the author's version of a work that was submitted to / accepted for publication.

Citation for final published version:

Attard, Gary Anthony, Hunter, Katherine, Wright, Edward, Sharman, Jonathan, Martínez-Hincapié, Ricardo and Feliu, Juan M. 2017. The voltammetry of surfaces vicinal to Pt{110}: structural complexity simplified by CO cooling. *Journal of Electroanalytical Chemistry* 793 , pp. 137-146. 10.1016/j.jelechem.2016.10.005

Publishers page: <http://dx.doi.org/10.1016/j.jelechem.2016.10.005>

Please note:

Changes made as a result of publishing processes such as copy-editing, formatting and page numbers may not be reflected in this version. For the definitive version of this publication, please refer to the published source. You are advised to consult the publisher's version if you wish to cite this paper.

This version is being made available in accordance with publisher policies. See <http://orca.cf.ac.uk/policies.html> for usage policies. Copyright and moral rights for publications made available in ORCA are retained by the copyright holders.





Contents lists available at ScienceDirect

Journal of Electroanalytical Chemistry

journal homepage: www.elsevier.com/locate/jelechem

The voltammetry of surfaces vicinal to Pt{110}: Structural complexity simplified by CO cooling

Gary A. Attard^{a,*}, Katherine Hunter^a, Edward Wright^b, Jonathan Sharman^b,
Ricardo Martínez-Hincapié^c, Juan M. Feliu^c

^a Cardiff Catalysis Institute, School of Chemistry, Cardiff University, Cardiff, CF10 3AT, UK

^b Johnson Matthey Technology Centre, Blounts Court Road, Sonning Common, Reading, Berkshire, RG4 9NH, UK

^c Instituto de Electroquímica, Universidad de Alicante, Apartado 99, E-03080, Alicante, Spain

ARTICLE INFO

Article history:

Received 27 July 2016

Received in revised form 30 September 2016

Accepted 3 October 2016

Available online xxx

Keywords:

Pt{110}

Cyclic voltammetry

Stepped surfaces

Electrosorption

ABSTRACT

By flame-annealing and cooling a series of Pt $n\{110\} \times \{111\}$ and Pt $n\{110\} \times \{100\}$ single crystal electrodes in a CO ambient, new insights into the nature of the electrosorption processes associated with Pt{110} voltammetry in aqueous acidic media are elucidated. For Pt $n\{110\} \times \{111\}$ electrodes, a systematic change in the intensities of so-called hydrogen underpotential (Hupd) and oxide adsorption voltammetric peaks (for two dimensionally ordered (1×1) terraces and linear $\{111\} \times \{111\}$ step sites) point to a lack of surface reconstruction with all surfaces adopting a (1×1) configuration. This is in contrast to hydrogen cooled analogues which give rise to significant residual surface disorder, probably associated with the excess 50% of atoms remaining atop of the surface upon deconstruction of the $\{110\} - (1 \times 2)$ terrace phase. In contrast, Pt $n\{110\} \times \{100\}$ stepped electrodes, when cooled in gaseous CO following flame-annealing, show a marked tendency towards surface reconstruction, even at low step densities. Variations in potential of the Pt{110}– (1×1) Hupd electrosorption peaks as a function of specific ion adsorption strength and pH point to weak specific adsorption for both anions (including perchlorate and fluoride) and cations (including Na^+ and K^+). CO charge-displacement measurements of the potential of zero total charge (PZTC) allow inferences to be made concerning the nature of the electrosorbed species in the hydrogen underpotential deposition (Hupd) region. Hence, a coherent interpretation of the complex voltammetric phenomena often displayed by platinum surfaces vicinal to the {110} plane is proposed.

© 2016 Published by Elsevier B.V.

1. Introduction

In a recent paper [1], the voltammetry of Pt{110} in aqueous perchloric acid and sodium hydroxide was reported. In agreement with previous studies [2,3], depending on the cooling environment after flame annealing, the surface of the electrode could be prepared in a partial (1×2) (nitrogen-cooled), (1×1) (CO-cooled) or “rough” (1×1) (hydrogen-cooled) state. In 0.1 M perchloric acid especially, a new voltammetric profile was observed in which the presence of long range, two dimensionally ordered Pt{110} terraces (after CO cooling) gave rise to singular Hupd/OH and oxide electrosorption features (Hupd in this context refers to Pt electrosorption peaks in the range 0.05–0.4 V versus RHE irrespective of whether or not they arise from hydrogen, OH or anion adsorption). Moreover, the electrocatalytic activity towards the oxygen reduction reaction (ORR) was found to differ significantly from previous reports which asserted that Pt{110} electrodes exhibit ORR activity equivalent to or greater than that of Pt{111} in

aqueous perchloric acid [4–8]. Rather, in reference [1], when all defects were eliminated from the electrode surface via CO cooling, ORR activity in aqueous perchloric acid was found unequivocally to be lower than that of Pt{111}.

Hence, we are undertaking an extensive re-evaluation of previous electrocatalytic studies involving Pt{110} and related surfaces since nearly all of these earlier investigations involved a flame-anneal/hydrogen cooling surface preparation protocol leading to the generation of defective surfaces [9–15]. Since ORR was shown previously to be highly sensitive to surface disordering, it was thought prudent to explore in a more controlled fashion the introduction of surface defects to a Pt{110}– (1×1) surface and its impact on surface voltammetry. To this end, the present manuscript is addressed. Future work will report findings relating to oxygen reduction, methanol electrooxidation and nitrate reduction.

A series of stepped Pt{110} surfaces have been prepared based on either {111} or {100} linear steps. By cooling these surfaces in CO following flame annealing, we hoped to compare and contrast with earlier results pertaining to hydrogen-cooled stepped surfaces [16,17]. It was hypothesised that the complexity associated with both terrace and

* Corresponding author.

E-mail address: attard@cardiff.ac.uk (G.A. Attard).

step reconstruction might be reduced or even eliminated using adsorbed CO, allowing for more detailed insights relating to the distinctive voltammetry of Pt{110}. In particular, the very broad and asymmetric Hupd electroreduction peak centred around 0.2–0.25 V (Pd/H) observed in aqueous perchloric acid [18,19] (we shall refer to this state from hence forth and throughout as the “classical Pt{110} terrace peak” or “Pct” for short) has posed an ongoing puzzle to surface electrochemists even since the earliest voltammetric measurements were performed [20]. More recently, Taguchi and Feliu asserted that Pct may be ascribed to “narrow” {111} terraces similar to those comprising the missing-row (1×2) reconstruction of Pt{110} [21]. This was because when Pt $n\{111\} \times \{111\}$ electrodes were studied using aqueous perchloric acid, a similar peak appeared for $n < 4$, i.e. the interaction of {111} steps at narrow terrace widths led to the generation of the “Pt{110}” 0.2–0.25 V feature. In contrast, Souza-Garcia et al. suggested that because the intensity of Pct grew with increasing values of n (using Pt $n\{110\} \times \{111\}$ electrodes) that it was probably associated with the average terrace width of the {110} terraces themselves meaning that the Pt $n\{111\} \times \{111\}$ surfaces at small values of n are reconstructed and therefore, must contain narrow {110} terraces [17]. In situ XRD investigations by Hoshi and co-workers [22] have demonstrated that Pt{331} (Pt $3\{111\} \times \{111\}$ or Pt $2\{111\} \times \{110\}$ in microfacet notation) remains in its unreconstructed (1×1) state after flame annealing and cooling in a hydrogen/argon environment supporting the view that narrow {110} terraces are not formed and that “splitting” of the {110} Hupd step peak for $n < 4$ into two components (using perchloric acid electrolyte) seems more linked to step-step interactions. Interestingly, a similar “splitting” of the {111} \times {100} step feature around the turning point of the stereographic triangle travelling from the {111} pole to the {100} pole (Pt{211}, Pt{311} and Pt{511} surfaces) is also observed in perchloric acid electrolytes [23], presumably again due to step-step interactions. However, the expectation of a splitting of the Hupd electroreduction peak associated with closely spaced steps is not fulfilled for small n either using Pt $n\{110\} \times \{100\}$ or Pt $n\{100\} \times \{110\}$ electrodes [16,24] (i.e. travelling along the stereographic triangle from the {100} pole to the {110} pole). In this case, evidence in support of such step sites being rather unstable has been put forward such that reconstruction of steps probably occurs [24]. In what follows, we shall explore this aspect in detail and moreover, suggest a new model that will interpret the complex voltammetry of surfaces vicinal to Pt{110} in terms of differing degrees of surface order resulting from particular annealing/cooling steps together with intrinsic structural instabilities associated with the presence of {110} \times {100} step sites.

2. Materials and methods

Work was carried out in both Cardiff and Alicante using the standard electrochemical and preparation and analytical procedures operative at both Universities. These procedures have been documented previously [25,26]. All stepped platinum {110} single-crystal electrodes were prepared using the method of Clavilier [27]. Considering that the electrodes were prepared and the experiments performed at two sites, the voltammetry displayed by each Miller index plane was remarkably similar and was also in accordance with previously published work [16,17]. There were some differences found between the Pt $n\{110\} \times \{100\}$ samples produced at both Universities and these will be discussed later. Electrodes were flame annealed and cooled in a CO (AIR LIQUIDE, N47) or H₂ (ALPHAGAZ, 99,999%) ambient (via a gas bubbler enclosure containing ultra-pure water saturated with CO or hydrogen) depending on the nature of the surface required [1–3]. 0.1 mol dm^{−3} HClO₄ and 0.1 M H₂SO₄ electrolyte solutions were prepared by dilution of high purity reagents (HClO₄, 70% Suprapur® supplied by Merck and H₂SO₄ Aristar 95%) in ultra-pure Milli-Q water with resistivity of >18.2 MΩ·cm. Buffer solutions were prepared by mixing HClO₄ and NaF (Merck, Suprapur®) to avoid specific adsorption and achieve more alkaline pHs [28]. Methanesulphonic acid (MSA) was purchased from Merck

(≥99%). Electrolytes were sparged with high purity nitrogen or argon for half an hour to remove dissolved carbon dioxide and oxygen prior to the collection of each set of voltammetry measurements. All potentials are reported with respect to a reversible hydrogen electrode scale although measurements collected at Cardiff utilised a palladium-hydrogen electrode in direct contact with the electrolyte [25].

3. Results and discussion

3.1. Voltammetry of Pt $n\{110\} \times \{111\}$ electrodes cooled in CO after flame anneal

In Fig. 1, a series of cyclic voltammograms for flame annealed and CO-cooled Pt $n\{110\} \times \{111\}$ surfaces in 0.1 M aqueous perchloric and sulfuric acid are shown. As reported previously [1], for Pt{110} in perchloric acid, the so-called Hupd region from 0.3 to 0.05 V is rather complex containing numerous reversible electroreduction peaks centred at 0.25, 0.20 and 0.145 V (Fig. 1A). In reference [1], all of these were associated with the presence of extended Pt{110}-(1×1) domains since electroreduction into the oxide peak at 1.1 V (electrochemical surface roughening) caused the attenuation and broadening of all peaks such that the CV would subsequently resemble a hydrogen-cooled electrode.

As the surface density of {111} steps is steadily increased, it is apparent that a systematic decrease in Hupd and oxide peak intensity ascribable to Pt{110} terraces is observed but no change in peak potential, general shape or width except for Pt{331}. This is consistent with maintenance of Pt{110} terrace symmetry. A peak appearing at 0.90 V as step density increases is ascribed by ourselves to electroreduction of oxide at

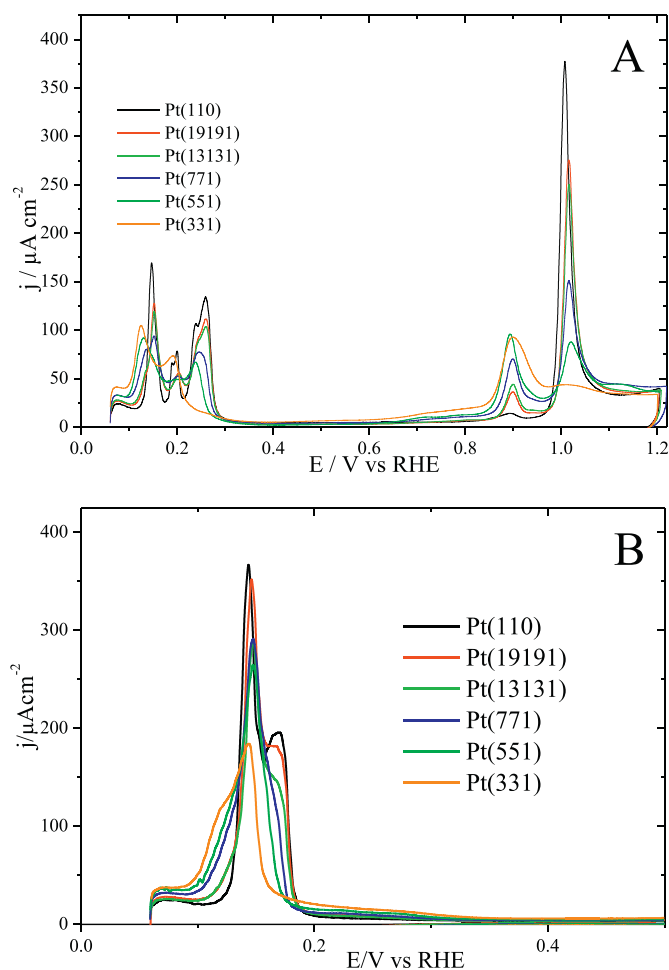


Fig. 1. Cyclic voltammograms of Pt $n\{110\} \times \{111\}$ electrodes in (A) 0.1 M aqueous perchloric acid and (B) 0.1 M sulphuric acid. Sweep rate = 50 mV/s.

the $\{111\} \times \{111\}$ linear step site. In fact Fig. 2 shows linear relationships between terrace and step oxide peak electroadsorption charges as a function of step surface density. This behaviour is in accordance with expectations based on a hard sphere model of an unreconstructed Pt surface. Furthermore, an isopotential point is observed at 0.12 V in which the peak at 0.145 V transforms into a peak centred at 0.12 V (see Pt{331} in particular). The Pt{331} CV is interesting because the peak at 0.20 V, previously ascribed to either narrow $\{111\}$ terraces [21] or $\{110\}$ reconstructed facets [17] is clearly well separated in potential from the Pt{110} terrace feature at 0.25 V, also as expected from the fact that Pt{331} represents a turning point whereby step and terrace sites become indistinguishable. In addition, significant peak broadening for oxide electroadsorption at the step (0.90 V) (which is correlated with the appearance of the 0.20 V peak) is speculated to arise from step-step interactions for narrow average terrace widths close to the turning point of the zone. It should also be noted that for Pt{331}, the oxide peak associated with Pt{110} terraces at 1.1 V has almost completely vanished. If Pt{110} terraces were present, both the 0.25 V and 1.1 V peaks should also be visible for Pt{331}.

Weaker and more subtle changes observed in Fig. 1A would include charge growing between 0.60 and 0.85 V which is ascribable to "OH" (in fact, the beginning of Oupd, which is more complex than Hupd for obvious reasons) adsorption on narrow Pt{111} terraces. As reported previously, when Pt $n\{111\} \times \{110\}$ surfaces are considered for $n > 2$, this charge component continues to grow as the average $\{111\}$ terrace width increases [21]. The corresponding development in the (well-separated) Hupd Pt{111} charge is still visible for Pt{331} as signified by a weak, rising current density from 0.30 to 0.20 V but is obscured by the larger, 0.20 V peak at more negative potentials. We shall see later in sulphuric acid that this feature becomes much more marked. Hence, we conclude that all surfaces vicinal to Pt{110} containing $\{111\}$ linear steps remain unreconstructed when prepared via CO cooling and for Pt{331}, this suggestion is in accordance with previous in situ XRD measurements [22].

In contrast, in reference [17] in which hydrogen-cooled Pt $n\{110\} \times \{111\}$ voltammetry was investigated, only the broad and asymmetric Pct feature centred at 0.25 V was reported which gradually diminished in magnitude with a slight shift to more negative potentials as surface step density increased. A gradual increase in the peak intensity associated with steps (at 0.12 V) was also observed. Clearly, in terms

of 2D Pt{110} terrace order, all hydrogen-cooled samples failed to sustain the presence of a 0.25 V 2D ordered terrace peak (although there is good overlap with Pct for Pt{110} in particular) and therefore, these samples must be intrinsically disordered relative to CO-cooled analogues. The nature of the broadness of Pct is speculated to stem from the presence of narrow $\{111\}$ terraces as residuals left over upon lifting of the (1×2) terrace reconstruction (electroadsorption charge at the more negative potential of Pct) and perhaps a variable number of relatively (compared to CO-cooled substrates) narrow Pt{110} terraces (at the more positive potential range Pct). This explanation accounts for the influence of both step-step interactions and residual Pt{110} 2D order leading to an increase in peak magnitude of Pct as step density diminishes. The nature of the actual, adsorbed species constituting this unusual electroadsorption peak will be discussed later.

In Fig. 3, the voltammetry of Pt{332} and Pt{110} is compared. Pt{332} in microfacet notation corresponds to Pt $6\{111\} \times \{111\}$ and the junction of the two $\{111\}$ sites corresponds to a $\{110\}$ linear step. This "step" feature gives rise to a well-defined voltammetric peak at 0.12 V when incorporated into Pt{110} and Pt{111} terrace sites [17, 21] and is clearly associated with 1D $\{110\}$ step order. It is evident from Fig. 3 that the 0.12 and 0.145 V peaks have different origins since even after varying the surface step density (including for hydrogen-cooled Pt{110}), the 0.12 V peak does not vary in potential so the 0.145 V peak reported here is unique and cannot be ascribed to $\{111\} \times \{111\}$ step sites. Rather, we assert that the 0.145 V peak is actually caused by electroadsorption on 2D Pt{110} terrace sites. The isopotential point at 0.12 V is then the result of a one to one correspondence between the number of 1D Pt{110} and 2D Pt{110} sites as step density is varied, again in accordance with a hard sphere interpretation of all surfaces being in their (1×1) unreconstructed state.

Fig. 1B also shows a family of CVs for CO-cooled Pt $n\{110\} \times \{111\}$ stepped surfaces in aqueous 0.1 M sulphuric acid. We have expanded the potential scale relative to Fig. 1A to show the Hupd peaks more clearly. Using a similar analysis to that described above, it is evident that the multiplicity of overlapping Hupd peaks is now confined to a much narrower range of potential as expected for more strongly specifically adsorbing anions such as sulphate. In fact for Pt{111} and after much discussion in the literature, sulphate rather than bisulphate has been demonstrated to be the specifically adsorbing species. We will assume hence forth that this is indeed true for Pt{110} [29–31]. The oxide

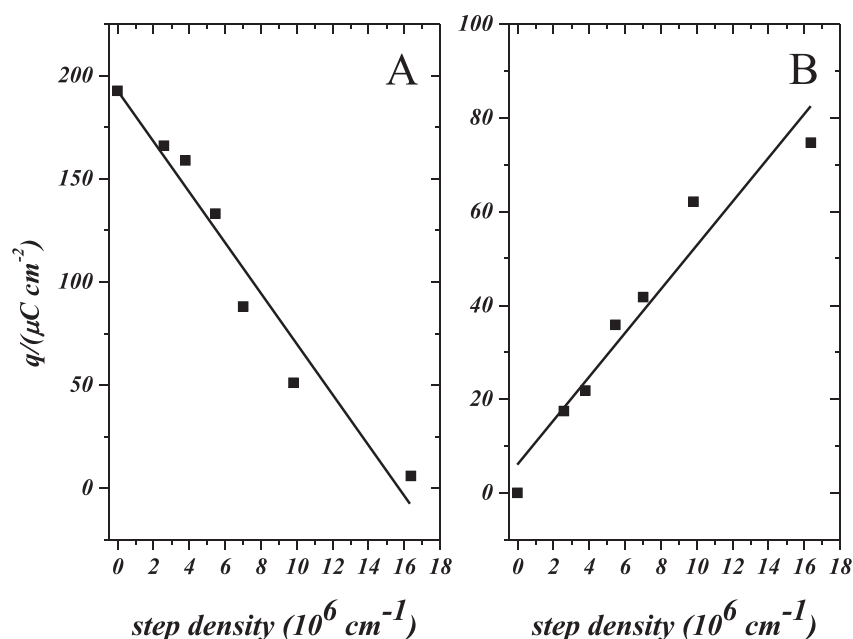


Fig. 2. Plots of Pt{110} (A) terrace and (B) $\{111\} \times \{111\}$ step oxide electroadsorption charge as a function of step density for Pt $n\{110\} \times \{111\}$ electrodes in 0.1 M perchloric acid.

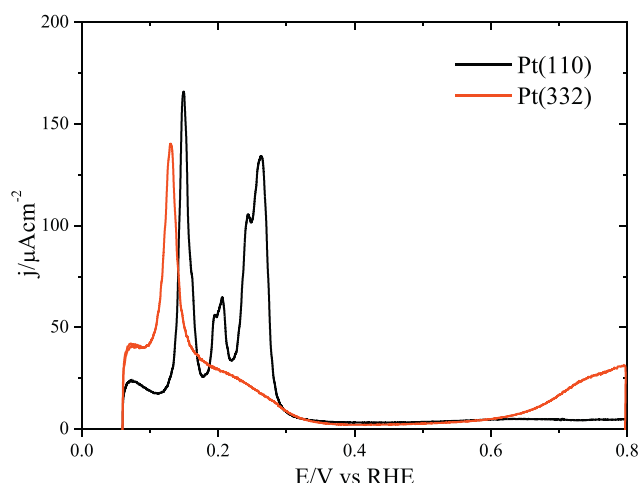


Fig. 3. Cyclic voltammograms of Pt{110}-(1 × 1) (black) and Pt{332} (red) in 0.1 M aqueous perchloric acid. Sweep rate = 50 mV/s.

electrosorption peaks also reflect the presence of specifically adsorbing sulphate anions relative to perchloric acid with peaks at 1.03 V and 0.92 V corresponding to electrosorption of oxide at terrace and step sites respectively (Supplementary Information Fig. S1). Fig. 4 shows how the charge under each of the oxide peaks is linearly correlated as a function of step density in agreement with previous assertions that all electrode surfaces exhibit a (1 × 1) terminated structure.

Returning to the Hupd potential region, if one assumes that the same electrosorption processes are occurring as for perchloric acid but confined within a narrower potential range, it is possible to make logical assignments concerning most of the features and suggest good candidates for the remainder. For example, the peak component at 0.17 V which is attenuated as step density is increased is almost certainly ascribable to the same process as was occurring in the 0.25 V peak in perchloric acid and is proposed to be a manifestation of long range Pt{110}-(1 × 1) 2D surface order. The correlated growth in the shoulder at most negative potentials (0.11 V) as step density increases must then be characteristic of 1D Pt{110} order (linear steps). Further progress can be made if Pt{331} voltammetry is scrutinised whereby the

electrosorption charge between 0.15 and 0.32 V together with a very broad feature between 0.5 and 0.8 V are considered together. Both of these may be positively identified as being due to Hupd and sulphate adsorption respectively on very narrow Pt{111} terraces [32]. In fact because the Pt{111} Hupd peak is identical in both sulphuric and perchloric acid, it is no surprise that the same potential range is exhibited by the Pt{331} “{111} terrace” contributions in both perchloric and sulphuric acids. Also, the slight shift to more positive potentials of the Pt{111} anion electrosorption charge upon changing from sulphuric to perchloric acid aqueous media is also in accordance with these peak assignments [33].

The more complicated issue arises from consideration of the intense peak centred 0.145 V. It is found to decrease in intensity (as step density increases) to about 50% of its original value in the case of the Pt{331} surface. Since Pt{331} contains no 2D ordered Pt{110} terrace sites, this 50% “residual” charge is ascribed to purely 1D Pt{110} order. Hence, two components of 1D Pt{110} may be discerned – a contribution at more negative potential (0.11 V) and one at more positive potentials (0.145 V). As a tentative suggestion (but see later PZTC data), we ascribe both peaks to essentially adsorption at Pt{110} 1D steps with (for positive potential sweep) cations desorbing in the peak at 0.11 V and anions adsorbing in the peak at 0.145 V. This demarcation of cationic and anionic charge separation overlapping with what is referred to classically as “hydrogen adsorption” has already been mentioned in relation to Pt{111} terraces. In a similar fashion, an interpretation of why for Pt{110}, the peak at 0.145 V is almost twice the size of that for Pt{331} could be that this “extra” charge is wholly caused by adsorption into 2D Pt{110} surface ordered sites which overlap with the step contribution. In this way, two contributions towards electrosorption at 2D Pt{110} ordered sites may also be delineated; that due broadly to anions at 0.16 V and that due broadly to cations at 0.145 V. A test of this hypothesis may be attempted by evaluations of PZTC as will be demonstrated later. The more important consequence of our hypothesis may be framed within the following:

Is it possible that all electrosorption at well-defined sites may ultimately be broken down into two contributions, anion adsorption at the more positive potential and cation adsorption at the more negative potential? The separation of these two processes would depend on the particular adsorption site, the relative strengths of anion and cation adsorption and the degree of lateral interaction occurring as each site is

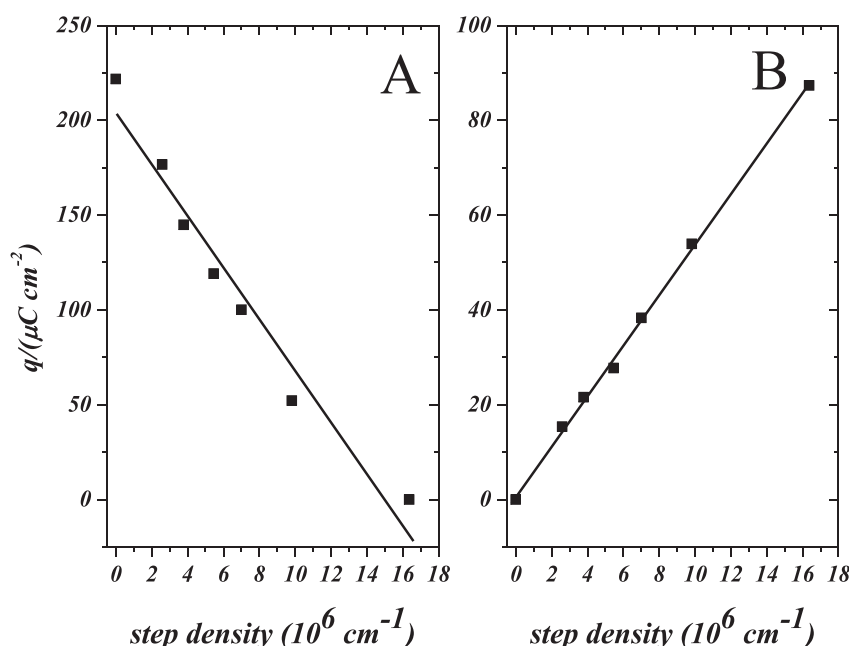


Fig. 4. Plots of (A) terrace and (B) step oxide electrosorption charge as a function of step density for Pt n{110} × {111} electrodes in 0.1 M sulphuric acid.

occupied. This happens with Pt(111) and Pt(100) in alkaline media [34]. Also, it should be noted that water interactions change with potential [35,36].

The notion of a local potential of zero charge has previously been discussed by [37,38]. This concept fits well the model being proposed in the present work in which a “patchwork” of locally charged states switch from negative to positive as a function of increasing potential and thus causing the generation of the various peaks recorded during CV (via adsorption/desorption of ions) depending on the sign of the excess charge at a specific site.

Looking back at the multiplicity of CV peaks seen for Pt{110} in perchloric acid, the 0.145, 0.20 and 0.25 V are all doublets and we suggest that each doublet may be seen as the cationic/anionic pair pertaining to 2D Pt{110} sites. However, the ratio of cations/anions in each state is predicted to change as the coverage of electrosorbed hydrogen changes (more sites for anion adsorption will become available as potential increases since more hydrogen leaves the surface and vice versa). This means that the 0.25 V peak would be largely dominated by the anionic component, the 0.145 V peak by the cationic component and the 0.20 V peak to a more equal distribution of cationic/anionic charges. That each of these peaks represents a different ratio of hydrogen/“OH” has already been suggested in [1] and is in line with recent thinking concerning the pH dependence of Hupd peaks at platinum electrodes [39]. This hypothesis will be tested further in Section 3.3.

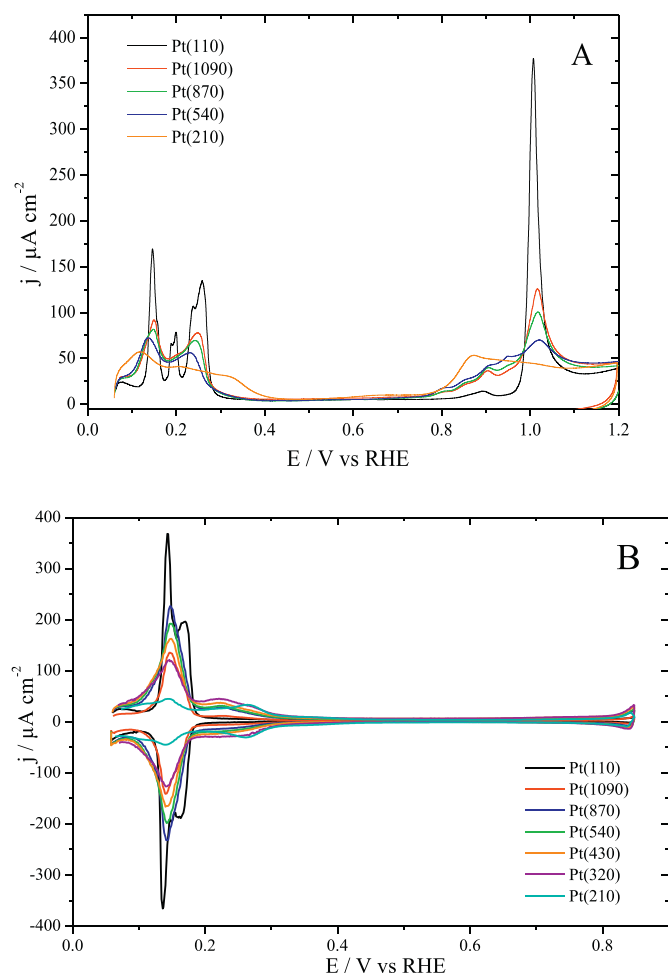


Fig. 5. Cyclic voltammograms of Pt $n\{110\} \times \{100\}$ electrodes in (a) 0.1 M aqueous perchloric acid and (b) 0.1 M sulphuric acid. Sweep rate = 50 mV/s.

3.2. Voltammetry of Pt $n\{110\} \times \{100\}$ electrodes cooled in CO after flame anneal

In Fig. 5A is shown the first voltammetric sweep from 0.05 to 1.2 V of freshly flame annealed and CO-cooled Pt $n\{110\} \times \{100\}$ electrodes in 0.1 M aqueous perchloric acid. In contrast to data depicted in Fig. 1A, inspection of Fig. 5A reveals that the introduction of {100} linear steps into the Pt{110} surface plane leads to voltammetry much more closely akin to hydrogen-cooled samples [16]. For example, what were well-defined doublets at 0.25 V and 0.145 V ascribable to the presence of 2D Pt{110} surface order, even at relatively low step density ($n = 10$) evolve immediately towards peaks that are much broader whilst simultaneously diminishing in intensity and shifting to more negative potentials. Moreover, the lack of a distinct isopotential point around 0.12 V is also noteworthy when compared with the data in Fig. 1A. It is striking that the 0.20 V doublet observed with CO-cooled Pt{110} is immediately quenched upon the introduction of step sites attesting to the surface structural sensitivity of this state.

The oxide electrosorption potential range between 0.8 and 1.2 V also changes in a less straightforward manner than for Pt $n\{110\} \times \{111\}$ stepped surfaces. Rather than observing two distinct and well-separated oxide adsorption peaks denoting step and terrace electrosorption, a multiplicity of adsorption peaks between 0.80 V and 0.90 V is evident. However, it is clear that the 0.89 V step adsorption peak (at Pt{111} \times {111} sites) is prominent amongst this complexity. Taking into account the absence of an analogous Pt{110} \times {100} oxide peak growing steadily with step density together with the presence of the 0.89 V peak (a symmetry that should not occur for this surface if it reflected a purely hard sphere (1×1) truncation of the platinum crystal), it is clear that the step sites are reconstructed. This would also be in accord with the lack of surface 2D order in the Hupd potential region alluded to above. The Pt{110}– (1×1) terrace peak at 1.1 V is observed to decrease as step density decreases until it completely vanishes for Pt{210}, as expected since Pt{210} is the turning point of the zone. Interestingly, the reproducibility between Cardiff and Alicante Pt $n\{110\} \times \{100\}$ substrates was also found to be less marked here with Cardiff samples displaying a slightly larger 0.89 V oxide step peak than those depicted in Fig. 5A. This was probably due to minute differences in the alignment of the cutting plane which possibly tipped the reconstruction direction towards the formation of {111} \times {111} steps for the Cardiff electrodes (Fig. S2). Irrespective of the number of {111} \times {111} steps formed after step reconstruction, the model being proposed is completely consistent with previous work by Garcia-Araez et al. demonstrating reconstruction of {110} \times {100} steps to form {111} \times {111} structures for flame annealed and hydrogen-cooled stepped Pt{100} [24].

In addition, the rate at which the terrace oxide peak is attenuated is quite different to that observed in Fig. 1. This point is emphasised in Fig. 6 whereby a plot of the electrosorption charge associated with the Pt{110}– (1×1) terrace sites is plotted as a function of step density for both Pt $n\{110\} \times \{111\}$ and Pt $n\{110\} \times \{100\}$ electrodes. For all step densities up to $n = 2$, it is found that the terrace charge for Pt $n\{110\} \times \{100\}$ electrodes is consistently smaller than that for the analogous Pt $n\{110\} \times \{111\}$ stepped surface. It is concluded from this that for a specified step density, the long range order of the terraces is also influenced by the reconstruction of the steps and that overall 2D long range order is diminished relative to Pt $n\{110\} \times \{111\}$ planes.

Fig. 5B also highlights changes in Pt $n\{110\} \times \{100\}$ voltammetry occurring when perchloric acid is replaced by sulphuric acid. As remarked earlier, the effect of the more strongly specifically adsorbing anion is to narrow the potential range of Hupd response although in this case, the emergence of {111} \times {100} Hupd step sites is evident at 0.28 V (remember that {110} is actually a compound step in microfacet notation denoted {111} \times {111}). Again, the oxide electrosorption peaks are all shifted to slightly more positive potentials in sulphuric acid electrolyte with the Pt{110} terrace peak at 1.03 V and the {111} \times {111} step

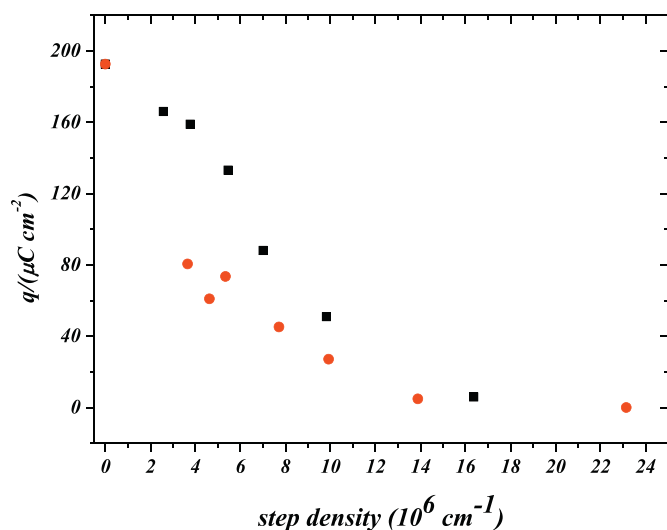


Fig. 6. Graph showing how the Pt{110} terrace oxide electrosorption charge in 0.1 M perchloric acid electrolyte varies as a function of step density for Pt n{110} × {111} electrodes (black) and Pt n{110} × {100} (red) electrodes.

peak situated at 0.93 V (especially prominent for Pt{10,9,0}) (see Supplementary Information Fig. S3). The increase in oxide peak intensity between 0.80 and 0.90 V is attributed to the presence of {110} × {100} steps although a comparison with this potential region in perchloric acid suggests quite a number of distinct adsorption sites are subsumed within this broad feature.

Unlike for Pt n{110} × {111} surfaces, the 0.17 V 2D Pt{110} terrace feature is immediately quenched for $n = 10$, a distinct 1D Pt{110} peak is absent at 0.11 V and a complete absence of an isopotential point for the Hupd peaks confirms that a simple hard sphere, (1 × 1) truncation of the bulk crystal would not fit with the data. Rather, charge observed at potentials negative of 0.14 V seems to be an off-shoot of the broadened 0.14 V peak discussed earlier. For Pt{210}, the emergence of Hupd charge in the potential range 0.30 to 0.45 V is consistent with the presence of narrow {100} terraces [40]. To summarise and encapsulate the influence of hydrogen/CO cooling on relative surface order, two exemplar CVs of stepped Pt{110} surfaces (Pt{19 19 1} and Pt{10 9 0}) are shown in Fig. S4.

3.3. Potential dependence of Hupd electrosorption peaks on specific adsorption strength and pH

In order to gain further insight into the electrosorbing species responsible for the principal 2D Pt{110} voltammetric peaks recorded for CO-cooled electrodes, CV data were collected in electrolytes containing anions of differing specific adsorption strength at almost constant pH, namely (bi)sulphate, fluoride, methyl sulphonate and perchlorate. Studies with methanesulphonic or trifluoromethanesulphonic acids illustrate the effect of non-adsorbing anions on the structure of interfacial water [41,42]. In addition, the pH dependence of the Hupd region of Pt{110} was investigated using a sodium fluoride buffer [28]. The data are shown in Fig. 7.

In Fig. 7A, the influence of different anions at almost constant pH is shown. The main change observed is a shift to more negative potentials of the 0.25 V peak. In reference [25], it was asserted that the Pct peak was associated with very weakly specifically adsorbing perchlorate anions influencing the electrosorption of an “OH” containing species. The presence of an OH containing species during the formation of the Pct electrosorption state has also been supported using PZTC and thermodynamic analyses [23]. In the present study, as the nature of the anion is changed, the systematic potential shift observed may be interpreted as more successful competition for adsorption sites by the more strongly specifically adsorbing anion. This interpretation has already been

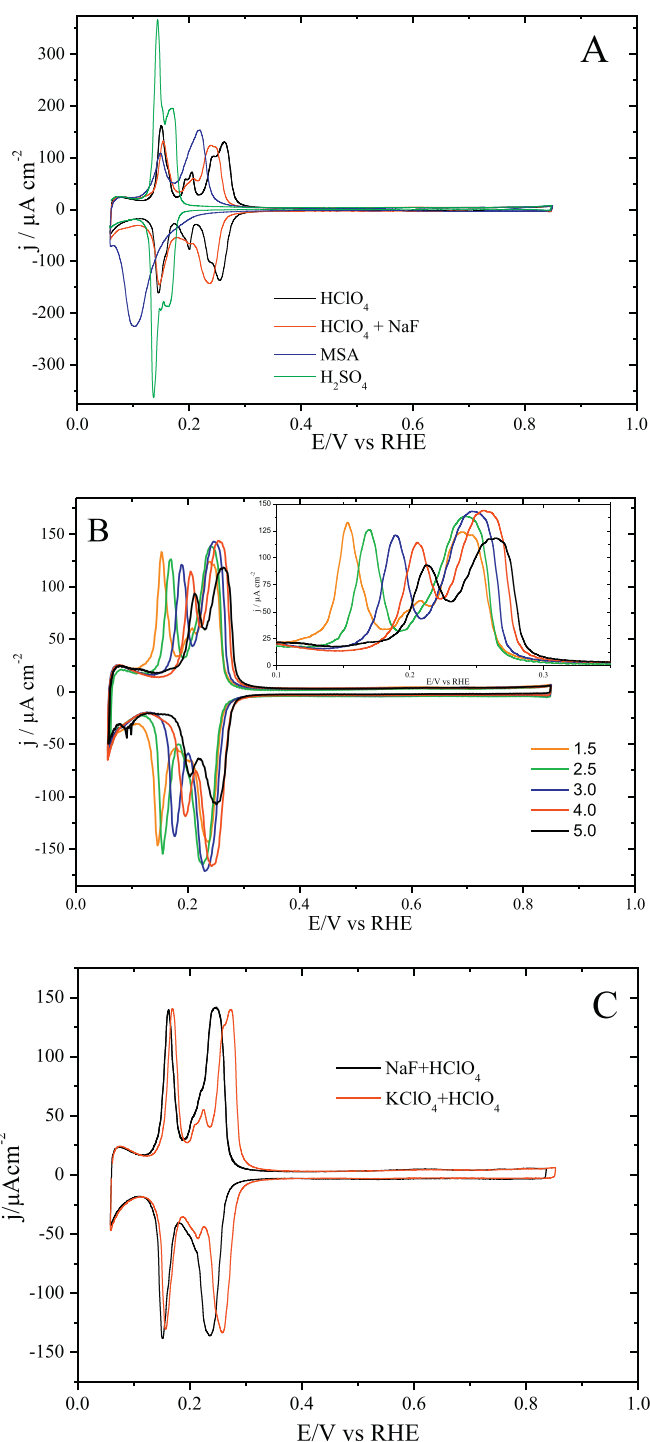


Fig. 7. Cyclic voltammograms of CO-cooled Pt{110} electrodes: (a) as a function of increasing anion adsorption strength (sulphate > methyl sulphonate > fluoride > “OH”); (b) as a function of pH; (c) at pH = 2 but using a NaF buffer (black) and unbuffered 0.01 M aqueous perchloric acid (red). Sweep rate = 50 mV/s.

used in the case of Pt{111} and Pt{100} [25] to explain marked potential shifts in the potential of anion adsorption and ultimately, complete blockage of any Pt-OH bond formation when sulphate is present. (This could be due to the anion effect on H₂O structure, chaotropic and kosmotropic effects, the anion itself only affects water environment and favours or hinders water supply to the surface [43]). The data in Fig. 7A therefore suggests that in terms of the strength of anion specific adsorption, the order of interaction is:

Sulphate > methanesulphonate > fluoride > perchlorate > “OH”

It is also noteworthy that the peak at 0.145 V hardly changes potential at all, irrespective of the nature of the anion indicating that the extent of anion adsorption at such negative potentials is rather small if not zero. This would be consistent with the potential of zero charge occurring at a value positive of 0.145 V (to anions at 0.145 V, the surface ostensibly bears a negative charge at all sites and therefore precludes electrosorption).

Thus, support for our initial assignment of the origins of the major Hupd 2D Pt{110} voltammetric peaks (mainly anion electrosorption at 0.25 V, mainly cation electrosorption at 0.145 V) is evident from these anion studies. However, an interesting and ongoing controversy relating to the nature of the adsorbing species in the Hupd region of Pt single crystal electrode surfaces may also be highlighted when the pH dependence of the peaks in Fig. 7B are scrutinised. For an RHE or Pd/H reference electrode, if the Hupd peaks corresponded to just proton electrosorption, there should actually be no pH dependence since the potential response should be strictly Nernstian. Since from Fig. 7B, this is clearly not the case an alternative interpretation of non-Nernstian effects needs to be formulated. One attempt to do this has been to assign non-Nernstian potential shifts in Hupd peaks as a function of pH to complex, non-stoichiometric combinations of H/OH/O adsorbing at for example step sites [39]. The problem with this interpretation is the inevitable co-existence (presumably at close proximity at the step) of H and OH on a platinum surface at room temperature which should spontaneously react to produce water according to previous ultra-high vacuum studies [44]. In [39], the authors did indeed note that on Pt{110} and Pt{100}, there is a small potential window in which H and OH co-exist on the surface, in what is traditionally called the “hydrogen region”. An explanation for this was discussed whereby the stronger bond of OH to these surfaces as compared to Pt{111}, in combination with the stabilization of OH provided by water, prevented the recombination of H and OH into water. It is true that H₂O stabilises OH but spontaneous formation of 2OH leads to facile and autocatalytic surface reactions with any H present to form water [45]. Hence, even in the presence of co-adsorbed water, the coexistence of H and OH on Pt at room temperature remains difficult to rationalise. We agree however that a co-adsorption of at least two species is responsible for a non-Nernstian shift in peak potential.

In the present study however, we suggest that differing degrees of specific adsorption of sodium ions and perchlorate anions in addition to hydrogen electrosorption may be used to interpret the data in Fig. 7B. This model is in agreement with very recent work by McCrum and Janik who used density functional theory to predict that the alkali metal cation potassium should specifically adsorb on Pt, especially for increasing pH [46] and in fact such coadsorption might be involved in the non-Nernstian shifts in Pt step peak potential. Much work has been undertaken by the Frumkin School in relation to the pH dependence of anion and cation adsorption [47]. From these studies, it was determined that the specific adsorption of anions and cations is pH dependent. An increase in pH leads to a weakening in the interaction of anions with an electrode surface and a strengthening in the interaction of cations and vice versa. This corresponds in a shift to more negative potentials in the PZC as anion adsorption strength increases and a shift of PZC to more positive potentials as cation interaction strength increases.

Hence, as pH increases, in Fig. 7B it is observed that the peak at 0.145 V shifts positively at a rate of 18 mV per pH unit and the 0.25 V peak at a rate of 6 mV per pH unit. The first peak shift of 18 mV per pH unit would be consistent with stronger interaction of the electrode with sodium cations requiring a more positive potential to cause desorption (PZC shifts to more positive potentials with increasing pH). The weakening in the interaction of fluoride anions (shift of PZC to more positive potentials) with the electrode surface as a function of increasing pH would then account for the 6 mV per pH unit positive shift observed for Pt{110}. The magnitudes of the potential shifts probably reflect a complex interaction between H/Na⁺ and “OH”/F[−]

competitively adsorbing at locally charged sites. In Fig. 7C, the influence of both anions and cations is combined for Pt{110} in 0.01 M aqueous perchloric acid and a pH = 2 sodium fluoride buffer. It is evident that since the pH is common to both electrolytes, the presence of Na⁺(aq) ions causes a slight shift in the 0.145 V peak to slightly more positive potentials and the F[−](aq) ions of the buffer engender a shift to more negative potentials in the potential of the 0.25 V peak (they compete more successfully than “OH” for the anion sites) as expected based on the model outlined above.

3.4. CO charge displacement measurements of the potential of zero total charge (PZTC)

In Fig. 8, CO charge displacement measurements of the potential of zero total charge (PZTC) are summarised as a function of step density for all surfaces. The total charge is the charge that would flow if all free charges (monopoles), dipoles and electrosorbed species (for example Pt–H) were stripped from the electrode surface. CO is an excellent chemisorbate for achieving this transformation (at least for potentials negative of its electrooxidation) and subject to a small correction, may provide a value of potential at which the ‘anionic’ and ‘cationic’ charge which flows upon exposure of Pt electrodes to CO are in perfect balance and thus, the PZTC is determined. Unfortunately, in most cases, the CO charge displacement method cannot separate the specific cationic and anionic charge flow contributions from individual local adsorption sites (steps, terraces and kinks). Rather, it may provide a ‘global average’ of all of these contributions although in the case of Pt{111}, because Hupd and anion electrosorption states are well separated, it is indeed possible to deduce the ‘definitive’ value of PZTC, i.e. for Pt{111}, the global value of PZTC is the same as the local value of PZTC [37,38]. This is important when surfaces such as Pt{110} in perchloric acid are considered because their voltammetry is manifested as a series of well-defined electrosorption states that span the entire Hupd potential range and if it is assumed that each electrosorption state reflects a varying surface charge as a function of potential, then the global PZTC determined using CO charge displacement may not reflect these locally charged states. However, it is logical to assume that at potentials well removed from the PZTC that the direction of transient current flow should reflect the majority charge species (cationic or anionic). Hence, close inspection of Fig. 8 indicates that not only is the PZTC both structure and anion sensitive but that certain electrosorption peaks must be dominated by one type of charge. For example, for Pt{110} in

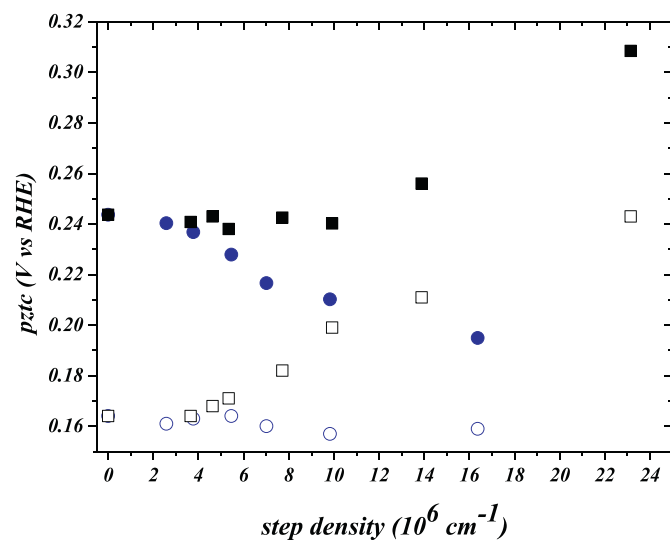


Fig. 8. Potential of zero total charge (PZTC) as a function of step density in 0.1 M aqueous sulphuric acid (open symbols) for Pt n{110} × {111} electrodes (circles) and in 0.1 M aqueous perchloric acid (full symbols) for Pt n{110} × {100} electrodes (squares).

perchloric acid, the PZTC coincides with the top of the more negative peak of the 0.25 V doublet designated P5 (from henceforth, all peaks will be labelled according to [1] with P1 signifying the most negative Hupd peak and P6 signifying the most positive). This would broadly indicate that P6 may be ascribed to the electrosorption of anions and those negative of this potential to desorption of cations. This would be in accordance with measurements recorded as a function of pH and varying the sequence anion/cation highlighted previously. However, if all peaks P1 to P6 do correspond to differentially charged states, it should also be possible to calculate the PZTC without having to undertake CO charge displacement.

3.4.1. PZTC evaluation without charge displacement

Fig. 9 shows a typical Pt{110} CV in 0.1 M perchloric acid with appropriate curve fitting using six Lorentzian peaks. Table 1 shows the values of deconvoluted charge according to each peak contribution. Also highlighted in the figure are three local values of PZC centred at each doublet (see earlier). According to this scheme, peaks P1, P3 and P5 would then correspond to cationic charge states and peaks P2, P4 and P6 to anionic charge contributions. At the “global” PZTC (evaluated using CO charge displacement), it is evident that P1 and P3 would correspond to “empty states” since the global PZTC is positive of both local PZC for these sites (cations in these sites see a locally positively charged surface so are repelled). However, the corresponding P2 and P4 peaks for analogous reasons should be “filled” with anions (as stated previously, sites exhibit an excess positive charge attracting the anions). The PZTC being at the potential of peak P5 means that only 50% of this cation charge site will be occupied together with 6% of the anionic peak P6. Therefore, if this breakdown of charge contributions is correct, it is evident that in terms of charge at the PZTC:

$$P2 + P4 + 0.06 \times P6 = 0.5 \times P5$$

Putting in the values of these “local” charges (in $\mu\text{C cm}^{-2}$) from Table 1:

$$P2 + P4 + 0.06 \times P6 = 4.6688 + 14.4192 + 0.06 \times 52.7804 = 22.2548$$

And

$$0.5 \times P5 = 0.5 \times 45.838 = 22.919$$

This remarkable agreement between the predicted condition of global PZTC and the actual value of PZTC determined experimentally lends further support to our peak assignments. Additionally, in future work it should be possible to reconstruct each CO charge transient as a function of potential using such analyses whereby electrosorption peaks may be assigned to positive and negative charge contributions, deconvoluted to determine their magnitudes and then combined as a function of potential (filling and emptying of each state). This analysis is currently being undertaken for other platinum single crystal electrode surfaces in order to generate PZTC values a priori and this will be the

Table 1
Deconvoluted charge for Pt{110} in 0.1 M HClO₄.

Peak	Charge ($\mu\text{C cm}^{-2}$)
1	−61.6136
2	−4.6688
3	−7.837
4	−14.4192
5	−45.836
6	−52.7804

subject of a subsequent publication. However, in the present study all measurements seem to point towards a consistent model involving adsorption/desorption of varying amounts of cations and anions depending on pH, anion/cation adsorption strength and surface structure.

3.4.2. Trends in PZTC of stepped Pt{110} electrodes

Returning to Fig. 8, the most striking feature of this PZTC data is the disparity in the trends depending on the nature of the step site. For example, in perchloric acid, increasing surface density of {110} \times {111} steps results in a steady shift to more negative potentials in the value of PZTC. In contrast, for {110} \times {100} stepped surfaces, after an initial steady plateau region, for narrow terraces, the PZTC shifts to more positive values. Within the model outlined above concerning locally charged sites, the shift to more negative potentials in PZTC as n decreases for Pt n {110} \times {111} may be ascribed to a decrease in the intensity of the 0.25 V doublet terrace peak corresponding to P5 and the large P6 anion peak. Since $P6 > P5$, this means that according to the definitions outlined above, the global PZTC value must shift to more negative values.

For the more complicated and reconstructed Pt n {110} \times {100} stepped surfaces, it is not straightforward to separate the various charge contributions, especially for Pct. However, the gradual decrease in the intensity of this peak that is observed as the average terrace width decreases might have also resulted in a steady shift in the PZTC to more negative potentials. However, from Fig. 4 it is noted that new Hupd electrosorption states begin to appear between 0.2 and 0.4 V for $n < 4$. It is speculated that it is the (larger) anion desorption charge in these states that pushes the PZTC to more positive values. This trend of increasing global PZTC is even more pronounced using sulphuric acid electrolyte since the Pt{110} Hupd states are confined to a narrower, more negative potential region due to specific adsorption of sulphate and the new Hupd states appearing at more positive potential due to {100} steps are much less affected by specifically adsorbing anions. This means that the almost static PZTC observed for lower step densities in perchloric acid is not realised in sulphuric acid electrolyte and rather, a gradual shift to more positive values in the PZTC is seen at all step densities. For Pt n {110} \times {111} stepped surfaces in sulphuric acid, the almost negligible change in the value of PZTC reflects the narrow confinement of all Hupd peaks within a narrow potential range and therefore, relative changes in step/terrace contributions make very little difference to the overall PZTC.

Compared to previous reports for hydrogen-cooled stepped samples [16,17], the trends reported in Fig. 8 are remarkably similar. The only major difference is a slight off-set in the PZTCs of the CO-cooled samples by approximately 10–15 mV to more positive potentials. This probably reflects the slightly greater degree of disorder present in the hydrogen-cooled samples.

4. Conclusions

A comprehensive electrochemical study of CO-cooled single crystal electrodes vicinal to the Pt{110} basal plane has been undertaken. Based on detailed analysis of electrosorption charges/voltammetry, pH, anion and cation effects and PZTC it is concluded that Pt n {110} \times {111} electrodes are unreconstructed and afford systematic variations in Hupd and electrosorbed oxide CV peaks as a function of

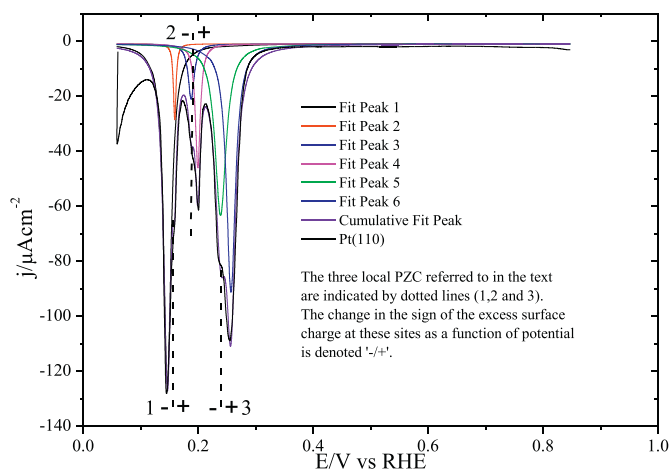


Fig. 9. Curve fitting to the 0.85 V to 0.05 V potential sweep of a Pt{110} – (1 \times 1) electrode in 0.1 M aqueous perchloric acid. Sweep rate = 50 mV/s.

step density. In contrast, similar analyses using Pt $n\{110\} \times \{100\}$ electrodes indicate a strong tendency towards surface reconstruction, not necessarily just confined to relatively unstable $\{110\} \times \{100\}$ steps but also possibly residual terrace sites adjacent to the steps. A new model of the Pt $\{110\}$ Hupd region is expounded in which local charged states that vary as a function of potential, pH and ionic adsorption are thought responsible for the variety of CV response recorded. The model allows for interpretation of non-Nernstian shifts in peak potential as a function of pH and the nature of the ions in contact with the electrode surface and points to weak specific adsorption of sodium ions and fluoride anions on Pt $\{110\}$ together with “OH” and the more usual hydrogen electrosorption. Moreover, it is asserted that by assigning “cationic” and “anionic” contributions to the overall Hupd region, one may evaluate the global value of the PZTC without the need of measuring CO charge displacement. The possibility that this model may apply generally to other well-defined Pt electrodes will be the subject of future investigations.

Acknowledgements

GAA acknowledges the financial support of the EPSRC towards a studentship for KH. RMH thankfully acknowledges support from Generalitat Valenciana under the Santiago Grisolia Program (GRISOLIA/2013/008). Partial support from MINECO (Spain) Project CTQ 2013-44083-P is greatly acknowledged.

Appendix A. Supplementary data

Supplementary data to this article can be found online at <http://dx.doi.org/10.1016/j.jelechem.2016.10.005>.

References

- [1] G.A. Attard, A. Brew, Cyclic voltammetry and oxygen reduction activity of the Pt $\{110\} - (1 \times 1)$ surface, *J. Electroanal. Chem.* 747 (2015) 123–129.
- [2] N.M. Marković, B.N. Grgur, C.A. Lucas, P.N. Ross, Surface electrochemistry of CO on Pt $\{110\} - (1 \times 2)$ and Pt $\{110\} - (1 \times 1)$ surfaces, *Surf. Sci.* 384 (1) (1997) L805–L814.
- [3] L.A. Kibler, A. Cuesta, M. Kleinert, D.M. Kolb, In-situ STM characterisation of the surface morphology of platinum single crystal electrodes as a function of their preparation, *J. Electroanal. Chem.* 484 (1) (2000) 73–82.
- [4] J. Perez, H.M. Villullas, E.R. Gonzalez, Structure sensitivity of oxygen reduction on platinum single crystal electrodes in acid solutions, *J. Electroanal. Chem.* 435 (1) (1997) 179–187.
- [5] N.M. Marković, R.R. Adžić, B.D. Cahan, E.B. Yeager, Structural effects in electrocatalysis: Oxygen reduction on platinum low index single-crystal surfaces in perchloric acid solutions, *J. Electroanal. Chem.* 377 (1) (1994) 249–259.
- [6] M.D. Maciá, J.M. Campiña, E. Herrero, J.M. Feliu, On the kinetics of oxygen reduction on platinum stepped surfaces in acidic media, *J. Electroanal. Chem.* 564 (2004) 141–150.
- [7] A. Kuzume, E. Herrero, J.M. Feliu, Oxygen reduction on stepped platinum surfaces in acidic media, *J. Electroanal. Chem.* 599 (2) (2007) 333–343.
- [8] H. Tanaka, Y. Nagahara, S. Sugawara, K. Shinohara, M. Nakamura, N. Hoshi, The influence of Pt oxide film on the activity for the oxygen reduction reaction on Pt single crystal electrodes, *Electrocatalysis* 5 (4) (2014) 354–360.
- [9] F. Colmati, G. Tremiliosi-Filho, E.R. Gonzalez, A. Berna, E. Herrero, J.M. Feliu, Surface structure effects on the electrochemical oxidation of ethanol on platinum single crystal electrodes, *Faraday Discuss.* 140 (0) (2009) 379–397.
- [10] S. Taguchi, J.M. Feliu, Kinetic study of nitrate reduction on Pt $\{110\}$ electrode in perchloric acid solution, *Electrochim. Acta* 53 (10) (2008) 3626–3634.
- [11] T.H.M. Housmans, A.H. Wonders, M.T.M. Koper, Structure sensitivity of methanol electrooxidation pathways on platinum: an on-line electrochemical mass spectrometry study, *J. Phys. Chem. B* 110 (20) (2006) 10021–10031.
- [12] F.J. Vidal-Iglesias, N. García-Arárez, V. Montiel, J.M. Feliu, A. Aldaz, Selective electrocatalysis of ammonia oxidation on Pt $\{100\}$ sites in alkaline medium, *Electrochem. Commun.* 5 (1) (2003) 22–26.
- [13] U. Müller, H. Baltruschat, Displacement of ethene and cyclohexene from polycrystalline Pt and Pt $\{110\}$ electrodes, *J. Phys. Chem. B* 104 (24) (2000) 5762–5767.
- [14] S.-G. Sun, A.-C. Chen, T.-S. Huang, J.-B. Li, Z.-W. Tian, Electrocatalytic properties of Pt $\{111\}$, Pt $\{332\}$, Pt $\{331\}$ and Pt $\{110\}$ single crystal electrodes towards ethylene glycol oxidation in sulphuric acid solutions, *J. Electroanal. Chem.* 340 (1) (1992) 213–226.
- [15] F. Cases, M. López-Atalaya, J.L. Vázquez, A. Aldaz, J. Clavilier, Dissociative adsorption of ethanol on Pt (h, k, l) basal surfaces, *J. Electroanal. Chem. Interfacial Electrochem.* 278 (1) (1990) 433–440.
- [16] J. Souza-Garcia, C.A. Angelucci, V. Climent, J.M. Feliu, Electrochemical features of Pt(S)[$n(110) \times (100)$] surfaces in acidic media, *Electrochem. Commun.* 34 (2013) 291–294.
- [17] J. Souza-Garcia, V. Climent, J.M. Feliu, Voltammetric characterization of stepped platinum single crystal surfaces vicinal to the (1 1 0) pole, *Electrochem. Commun.* 11 (7) (2009) 1515–1518.
- [18] J. Clavilier, R. Albalat, R. Gomez, J.M. Orts, J.M. Feliu, A. Aldaz, Study of the charge displacement at constant potential during CO adsorption on Pt $\{110\}$ and Pt $\{111\}$ electrodes in contact with a perchloric acid solution, *J. Electroanal. Chem.* 330 (1) (1992) 489–497.
- [19] J.M. Orts, A. Fernandez-Vega, J.M. Feliu, A. Aldaz, J. Clavilier, Electrochemical oxidation of ethylene glycol on Pt single crystal electrodes with basal orientations in acidic medium, *J. Electroanal. Chem. Interfacial Electrochem.* 290 (1) (1990) 119–133.
- [20] D. Armand, J. Clavilier, Electrochemical behaviour of the (110) orientation of a platinum surface in acid medium: the role of anions, *J. Electroanal. Chem. Interfacial Electrochem.* 263 (1) (1989) 109–126.
- [21] S. Taguchi, J.M. Feliu, Electrochemical reduction of nitrate on Pt(S)[$n(111) \times (1 1 1)$] electrodes in perchloric acid solution, *Electrochim. Acta* 52 (19) (2007) 6023–6033.
- [22] N. Hoshi, M. Nakamura, O. Sakata, A. Nakahara, K. Naito, H. Ogata, Surface X-ray scattering of stepped surfaces of platinum in an electrochemical environment: Pt $\{331\} = 3(111)-(111)$ and Pt $\{511\} = 3(100)-(111)$, *Langmuir* 27 (7) (2011) 4236–4242.
- [23] N. García-Araez, Enthalpic and entropic effects on hydrogen and OH adsorption on Pt $\{111\}$, Pt $\{100\}$, and Pt $\{110\}$ electrodes as evaluated by Gibbs thermodynamics, *J. Phys. Chem. C* 115 (2) (2011) 501–510.
- [24] N. García-Arárez, V.C. Climent, E. Herrero, J.M. Feliu, On the electrochemical behavior of the Pt(1 0 0) vicinal surfaces in bromide solutions, *Surf. Sci.* 560 (1–3) (2004) 269–284.
- [25] G.A. Attard, A. Brew, K. Hunter, J. Sharman, E. Wright, Specific adsorption of perchlorate anions on Pt(*hkl*) single crystal electrodes, *Phys. Chem. Chem. Phys.* 16 (27) (2014) 13689–13698.
- [26] J.M. Feliu, J.M. Orts, R. Gómez, A. Aldaz, J. Clavilier, New information on the unusual adsorption states of Pt $\{111\}$ in sulphuric acid solutions from potentiostatic adsorbate replacement by CO, *J. Electroanal. Chem.* 372 (1) (1994) 265–268.
- [27] J. Clavilier, D. Armand, S.G. Sun, M. Petit, Electrochemical adsorption behaviour of platinum stepped surfaces in sulphuric acid solutions, *J. Electroanal. Chem. Interfacial Electrochem.* 205 (1) (1986) 267–277.
- [28] R. Martínez-Hincapié, P. Sebastián-Pascual, V. Climent, J.M. Feliu, Exploring the interfacial neutral pH region of Pt $\{111\}$ electrodes, *Electrochem. Commun.* 58 (2015) 62–64.
- [29] Z. Su, V. Climent, J. Leitch, V. Zamylny, J.M. Feliu, J. Lipkowski, Quantitative SNIITRS studies of (bi)sulfate adsorption at the Pt $\{111\}$ electrode surface, *Phys. Chem. Chem. Phys.* 12 (46) (2010) 15231–15239.
- [30] N. García-Araez, V. Climent, P. Rodriguez, J.M. Feliu, Elucidation of the chemical nature of adsorbed species for Pt $\{111\}$ in H₂SO₄ solutions by thermodynamic analysis, *Langmuir* 26 (14) (2010) 12408–12417.
- [31] N. García-Araez, V. Climent, P. Rodriguez, J.M. Feliu, Thermodynamic evidence for K + SO₄²⁻ ion pair formation on Pt $\{111\}$. New insight into cation specific adsorption, *Phys. Chem. Chem. Phys.* 12 (38) (2010) 12146–12152.
- [32] A. Rodes, K. El Achi, M.A. Zamakhchani, J. Clavilier, Electrochemical Probing of Step and Terrace Sites on Pt [$N(111) \times (111)$] and Pt $[N(111) \times (100)]$, in: H.H. Brongersma, R.A. van Santen (Eds.), *Fundamental Aspects of Heterogeneous Catalysis Studied by Particle Beams*, Springer US, Boston, MA 1991, pp. 75–82.
- [33] J. Clavilier, The role of anion on the electrochemical behaviour of a $\{111\}$ platinum surface; an unusual splitting of the voltammogram in the hydrogen region, *J. Electroanal. Chem. Interfacial Electrochem.* 107 (1) (1979) 211–216.
- [34] R.M. Arán-Ais, M.C. Figueiredo, F.J. Vidal-Iglesias, V. Climent, E. Herrero, J.M. Feliu, On the behavior of the Pt(1 0 0) and vicinal surfaces in alkaline media, *Electrochim. Acta* 58 (2011) 184–192.
- [35] A.M. Gómez-Marín, J.M. Feliu, Thermodynamic properties of hydrogen–water adsorption at terraces and steps of Pt $\{111\}$ vicinal surface electrodes, *Surf. Sci.* 646 (2016) 269–281.
- [36] K. Schwarz, B. Xu, Y. Yan, R. Sundararaman, Partial oxidation of step-bound water leads to anomalous pH effects on metal electrode step-edges, *Phys. Chem. Chem. Phys.* 18 (24) (2016) 16216–16223.
- [37] G.A. Attard, O. Hazzazi, P.B. Wells, V. Climent, E. Herrero, J.M. Feliu, On the global and local values of the potential of zero total charge at well-defined platinum surfaces: stepped and adatom modified surfaces, *J. Electroanal. Chem.* 568 (2004) 329–342.
- [38] V. Climent, G.A. Attard, J.M. Feliu, Potential of zero charge of platinum stepped surfaces: a combined approach of CO charge displacement and N₂O reduction, *J. Electroanal. Chem.* 532 (1–2) (2002) 67–74.
- [39] M.J.T.C. van der Niet, N. García-Araez, J. Hernández, J.M. Feliu, M.T.M. Koper, Water dissociation on well-defined platinum surfaces: the electrochemical perspective, *Catal. Today* 202 (2013) 105–113.
- [40] F.J. Vidal-Iglesias, J. Solla-Gullón, J.M. Campiña, E. Herrero, A. Aldaz, J.M. Feliu, CO monolayer oxidation on stepped Pt(S) [$(n-1)(1 0 0) \times (1 1 0)$] surfaces, *Electrochim. Acta* 54 (19) (2009) 4459–4466.
- [41] A.P. Sandoval, M.F. Suárez-Herrera, V. Climent, J.M. Feliu, Interaction of water with methanesulfonic acid on Pt single crystal electrodes, *Electrochem. Commun.* 50 (2015) 47–50.
- [42] A. Berná, J.M. Feliu, L. Gancs, S. Mukerjee, Voltammetric characterization of Pt single crystal electrodes with basal orientations in trifluoromethanesulphonic acid, *Electrochem. Commun.* 10 (11) (2008) 1695–1698.
- [43] A. Berná, V. Climent, J.M. Feliu, New understanding of the nature of OH adsorption on Pt(1 1 1) electrodes, *Electrochem. Commun.* 9 (12) (2007) 2789–2794.

- [44] L.K. Verheij, Kinetic modelling of the hydrogen-oxygen reaction on Pt(111) at low temperature (<170 K), *Surf. Sci.* 371 (1) (1997) 100–110.
- [45] A. Michaelides, P. Hu, Catalytic water formation on platinum: a first-principles study, *J. Am. Chem. Soc.* 123 (18) (2001) 4235–4242.
- [46] I.T. McCrum, M.J. Janik, pH and alkali cation effects on the Pt cyclic voltammogram explained using density functional theory, *J. Phys. Chem. C* 120 (1) (2016) 457–471.
- [47] B.E.C. Peter Horsman, E. Yeager, *Comprehensive Treatise of Electrochemistry: The Double Layer*, Springer US, 1980 453 XIX.